

# Performance of New Generation of Engineered Concrete Materials in Infrastructure Applications

Khandaker M. A. Hossain  
*Ryerson University, Toronto, Ontario, Canada*  
*ahossain@ryerson.ca*

## Abstract

Engineered concrete (EC) is a new generation of high performance fibre reinforced composite material designed with micromechanical principles. The high strain capacity while maintaining low crack widths makes EC an ideal material for construction of sustainable infrastructure with high durability, ductility and energy absorbing capacity. This paper presents the structural performance of EC structural components in buildings and bridges. The structural performance of EC link slab in joint-free bridge deck construction and ECC beam-column building frames will be described based on their traditional concrete counterparts. The performance will be judged based on load-deflection response, stiffness, strain developments, crack characterization, failure modes, ductility and energy absorbing capacity.

## Keywords:

Engineered concrete, Link slab, Joint-free bridge deck, building frame

## 1. Introduction

Engineered concrete (EC) is a high performance fiber reinforced cementitious composites designed with micromechanical principals (Li and Kanda, 1998). Micromechanical design allows optimization of the EC for high performance, resulting in extreme tensile strain capacity while minimizing the amount of reinforcing fibers, typically less than 2% by volume. Unlike ordinary cement-based materials, EC strain-hardens after first cracking, similar to a ductile metal, and demonstrates a strain capacity 300 to 500 times greater than normal concrete. Even at large imposed deformation, crack widths of EC remain small, less than 60  $\mu\text{m}$ . Comprehensive research has been conducted over the years on EC commonly known as engineered cementitious composite (EC) incorporating supplementary cementing materials (SCMs) such as fly ash, slag, volcanic ash and metakaolin (Ozbay *et al.*, 2012; Hossain and Anwar, 2014 Sahmaran *et al.*, 2009; Wang and Li, 2007). Benefits of using SCMs, include reductions in energy consumption, greenhouse gas releases, and other pollutant emissions from initial mining of limestone, calcinations, and grinding in cement production.

Although mix design, mechanical and durability properties of EC have been investigated extensively, very limited research has been conducted on EC based structural elements especially for bridge and building infrastructures. Every year, in the world, billions of dollars are spent to repair and maintenance of bridge and building infrastructures. The poor durability of concrete structures throughout the world is an increasingly large concern. With decreasing budget allocations for infrastructure maintenance, rehabilitation, and replacement, the need for greater durability is superficial. High strength concrete has been used in maintenance and repair works of infrastructures (Li, 2003; Li *et al.*, 2002). But none of these

solutions target the inherent shortfall of concrete brittleness causing cracking which allows salt water to corrode reinforcing bars and finally leads to structural failure.

With intrinsically tight crack width and high tensile ductility, EC represents a new generation of high-performance concrete material that offers significant potential to naturally resolving the durability problem of reinforced concrete structures (Li, 2003). The combination of greener material, deterioration resistance, decreased maintenance and extended life cycle suggests that the sustainability of EC based infrastructure will be far superior to those with conventional concrete. Over the last 15 years, research at Ryerson University have been devoted to developing sustainable high performance concretes (including self-consolidating concrete ‘SCC’ and EC) and innovative structural systems/construction technologies (Hossain, 2013; Ozbay *et al.*, 2012; Hossain and Anwar, 2014; Sahmaran *et al.*, 2009; Hossain *et al.*, 2015). Design guidelines incorporating structural performance and serviceability of EC based structural elements are not available in Codes. Lack of research studies warrants investigations on to understand the structural behavior of EC based structural elements compared their conventional concrete counterparts in order to develop design guidelines and specifications.

This paper presents the structural performance of EC based structural components in building and bridge structures. A joint-free bridge deck concept using EC link slab connecting adjacent simply supported girders (Fig.1) replacing mechanical expansion joints (a major source of bridge deterioration requiring constant maintenance and replacement) can solve durability problems, extend service life and save millions of dollars (Alampalli and Yannotti, 1998; Gilani, 2001; Wolde-Tinsae and Klinger 1987; Caner and Zia, 1998; Lepech and Li, 2009). The use of EC based frame can also enhance the ductility, energy absorbing capacity and durability of framed building systems.

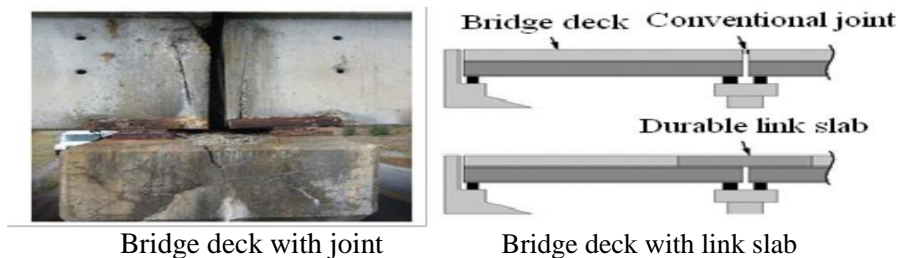


**Figure 1: Joint-free bridge deck with link slab**

The high strain capacity while maintaining low crack widths of EC make it an ideal material for the link slab and building frame application (Li, 1993; Li, 1998; Sahmaran *et al.*, 2010; Fischer and Li, 2003). Lack of research studies warrants extensive research investigations on structural performance of such EC based new structural systems for their implementation construction (Hossain *et al.*, 2015). The structural performance of EC based link slab in joint-free bridge deck construction and EC beam-column building frames will be described compared to their traditional SCC counterparts based on load-deformation response, stiffness, strain developments, crack characterization, failure modes, ductility and energy absorbing capacity.

## 2. Investigations

Comprehensive research consisting of experimental and theoretical investigations is in progress to study the structural performance of different types of building and bridge structural elements incorporating EC and other types of concretes under monotonic, cyclic and fatigue loading conditions. Experimental results of link slab (used for joint-free bridge construction) and one-story beam-column frame (for building construction) made of EC and a conventional SCC are the subject matter of this paper.

## 2.1 Investigation on Beam-Column Frame

Research had been conducted to study the behaviour of flexure critical reinforced beam-column frame subjected to in-plane monotonic lateral loading. Model frames of approximately 1/3<sup>rd</sup> scale were made using EC and control self-consolidating concrete (SCC). These flexure critical frames (designed with flexure and shear reinforcements) fixed at the base were tested to induce flexure dominated failure.

### 2.1.1 Geometric dimensions of frame specimens and reinforcement details

Model frames of approximately 1/3<sup>rd</sup> scale of prototype (having rectangular beam and column) were constructed and tested. Figure 2 shows a typical frame connected (fixed) to a strong base beam. Strong base beam footing was rigidly fixed to the strong floor of the Structural Laboratory. Figure 2 shows the geometric dimensions and reinforcement details of frames. 120 x 160 mm beams/columns having shear/tie (6 mm bar at 100 mm c/c) and main (4, 10 mm bar for beam and 4, 15 mm bar column) reinforcements were used (Fig. 2). The heavily reinforced strong base beam footing acted as a means to rigidly fix the frame at the base of the column. The base footing was 2210 mm long and 300 mm x 500 mm in cross-section. It had two 204 mm x 160 mm rectangular vertical holes to accommodate column to be rigidly fixed to the base. It also has four 40 mm dia vertical holes for connecting to the strong floor of the lab through threaded rods. It also had two 40 mm lateral holes to connect frame specimens to the base footing. Overall, the base beam footing served as a rigid support to frame at the bases of the column.

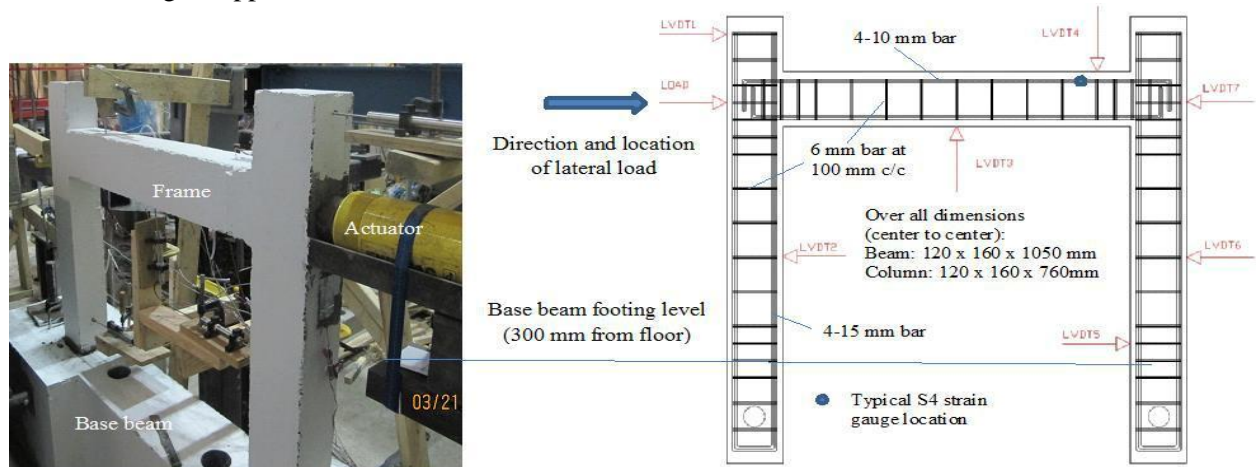


Figure 2: Typical beam-column frame and test set-up with instrumentation

### 2.1.2 Material properties and construction model frame

The materials used in the production of EC mixture were Type 10 Portland cement (ASTM Type I), fly ash, silica sand with 110  $\mu\text{m}$  average grain size, polyvinyl alcohol (PVA) fibers (with a diameter of 39  $\mu\text{m}$  and a length of 8 mm) and a polycarboxylic-ether type high-range water-reducing admixture (HRWRA). The EC mix had cement (C): fly ash (FA): silica sand ratio of 1:1.2: 0.80 by mass, 26  $\text{kg}/\text{m}^3$  of PVA, 5.4  $\text{kg}/\text{m}^3$  of HRWRA and water to binder (w/(C+FA)) ratio of 0.27. A commercial SCC consisted of 10 mm stone aggregate, sand, Portland cement, silica fume and air-entraining admixture was used. For each 30 kg pre-package bag, 2.4 liter of water was added and mixed to produce SCC.

Immediately after mixing, flowable SCC or EC was poured into wooden formwork and the frames were cast horizontally without any consolidation. Control specimens for each types of concrete in the form of cylinders and beams were also cast at the same time. All frames with control specimens were cured until the age of testing (for 28 days) using wet burlaps in the laboratory conditions with a relative humidity and temperature of  $50\% \pm 2.5\%$  and  $24 \pm 2^\circ\text{C}$ , respectively. Mean compressive and flexural strength of SCC at the age of testing were 50.6 MPa and 4.5 MPa, respectively while 63.5 MPa and 6.1 MPa, respectively for EC. The mean value of yield strength for 10 mm, 15 mm and 6 mm bars were 527 MPa, 478 MPa and 429 MPa, respectively while yield strain were 2240, 2310 and 2245 microstrain, respectively.

### 2.1.3 Frame instrumentation, test set-up and testing

Strain gauges were installed on the longitudinal (main) reinforcements and concrete surface at critical locations. Seven linear voltage displacement transducers (LVDTs) designated as (LVDT1 to LVDT7) were used to measure deflection as shown in Figure 1. The monotonic lateral loading was applied at the level of the beam by a hydraulic actuator at (test set-up shown in Figure 1) and loading continued until failure of frame specimens. During loading history, deflection and steel/concrete strain developments were recorded by a computer aided data acquisition system. The crack development and failure modes were visually observed during testing and crack's width was measured using a crack scope.

### 2.1.4 Analysis of structural performance of frames

Lateral load-top deflection (LVDT 7) curves are presented in Fig. 3(left). The slope change in the response indicated crack formation/initiation or yielding of reinforcing bars. EC frame exhibited 30% higher strength, 25.9% higher deflection and 46% higher column rotation than its SCC counterparts. Table 1 summarizes load, deflection and strain characteristics. The strength/load capacity enhancement seemed to be proportional to the % increase in concrete strength (EC compressive strength was 26.7% higher than SCC while tensile strength was 33% higher than SCC).

**Table 1: Summary of load-deflection and load-strain responses**

Frame	Load (kN) and deflection (mm)			Strain (micro-strain)			
	Ultimate/peak load	Ultimate lateral top deflection	Load (1 <sup>st</sup> crack)	Concrete tensile strain	Column rebar strain	Beam rebar strain	Concrete compressive strain
SCC	59.5	65.19	10	2295	926	1600	2435
EC	77.5	82.66	15	4020	1241	1776	3212

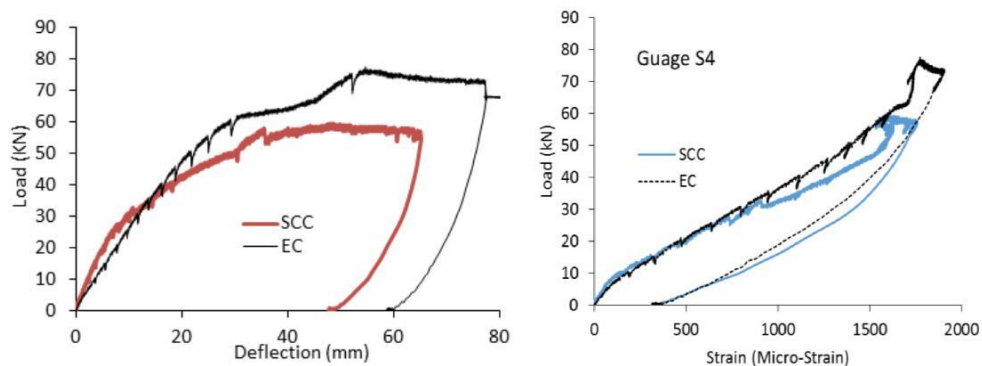


**Figure 3: Lateral load-top deflection and load-rebar strain responses of SCC/EC frame**

Initial stiffness and energy absorbing capacity (calculated as initial slope and area under the lateral load-deflection presented in Figure 2(left) up to 85% of the post-peak load, respectively) of the EC frame were 0.625 times lower and 3.35 times higher, respectively while its SCC counterpart. The displacement ductility (ratio of failure displacement at 80% of ultimate load at the post-peak descending part to the displacement at 80% of ultimate load at the pre-peak ascending part of the load-deflection response shown in Fig. 2-left) was 1.83 higher than its SCC counterpart. Low initial stiffness and high ductility coupled with good energy absorbing capacity, strain hardening and multi-cracking characteristics with tight crack width makes EC frame superior compared to SCC frames for construction applications.

Figure 2(right) shows typical comparison of flexural rebar strain development in SCC and EC frames with bars in EC frame showing higher strain development. The developed concrete compressive and tensile strains for EC frames were also higher than those of SCC frame (Table 1). Table 1 also shows that rebar strain in both column and beam did not reach yield strain for SCC and EC frames. Figure 4 shows the crack development and propagation in SCC/EC frames at failure. In general, cracking predominantly centered near the beam-column joint. Initiation of cracks started from the tension face of the beam near the joints (at around 10kN -15kN load) and propagated towards the compression zone as load

increased. Cracks (diagonal) were also extended to column in the joint regions. EC frame exhibited multiple micro-cracking behavior showing extensive hairline cracks in the beams and columns. SCC frames did not show multiple micro-cracking behavior and the zone of cracking is very limited compared to EC with no crack formation along the height of the column or beam length. SCC/EC frames failed due to flexure failure of beam at the joint exhibiting the formation of a major crack extended from the tension face to compression face as shown in Figure 4. Maximum crack widths were limited to 1.8 mm and 0.023mm at failure for SCC and EC frame, respectively. For the frames major cracks were developed in beam near the beam-column joint because of higher moment of inertia in the column. As such, failure due to beam flexure was expected due to weak beam-strong column design concept used in this study which is normally adopted in practical construction.

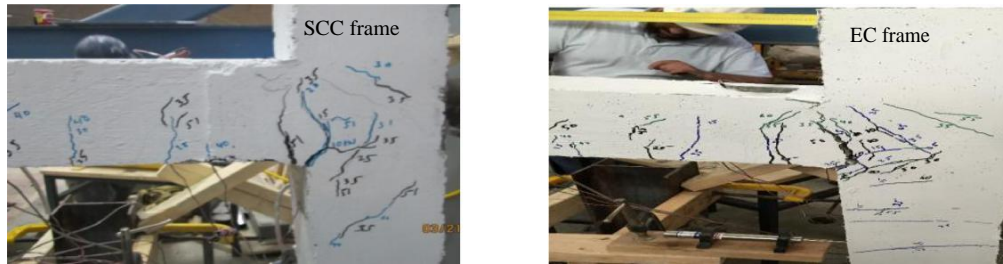


**Figure 4: Crack development and failure mode of SCC and EC frames**

## 2.2 Investigation on Link Slab

The deformed shape and moment distribution due to applied load of a two-span bridge structure with link slab (including an enlarged view of the link slab portion) are schematically shown in Fig. 5(left). Flexural crack formation was expected at the top of the link slab. Link slab specimens were designed to include the distance between the points of inflection in the adjacent spans. The location of inflection point (depending on the stiffness of the link slab) varies between 0 and 20% of the span length.

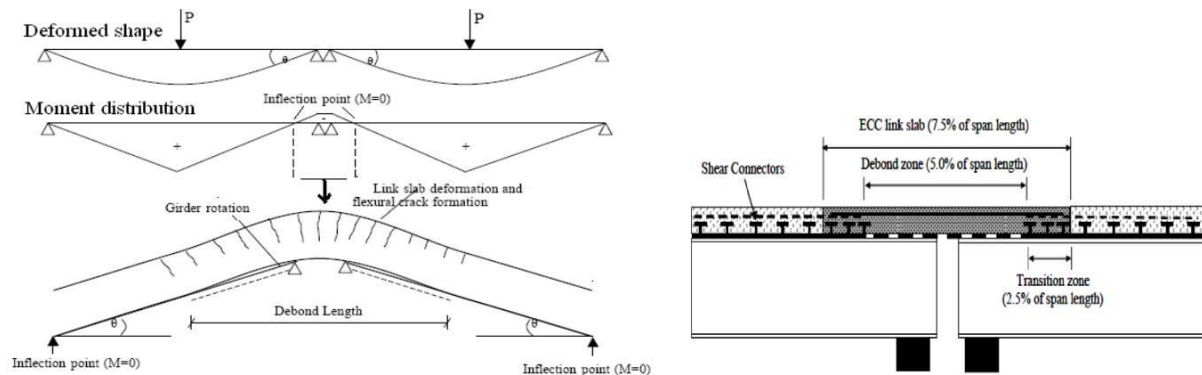


**Figure 5: Two span bridge showing link slab deformation and link slab showing components**

### 2.2.1 Geometric dimensions, materials and casting of tested link slabs

Fig. 5(right) shows the components of a typical link slab. The length of the debond zone (throughout which all shear connectors are removed and a debonding mechanism is placed) is 5.0% of each adjacent bridge span. The length of the link slab is extended 2.5% further into each adjacent span (known as transition zone) to help transfer load from the girders into the link slab through additional shear connectors (Caner and Zia 1998, Lepech and Li, 2009; Zia et al. 1995). Model SCC/EC link slab specimens of 1/4<sup>th</sup> scale were tested as shown in Fig. 6. The dimensions of the representative full-scale bridge deck were 711 mm (width) and 230 mm (depth). Based on this, a typical 1/4 scale link slab model had a total length of 930 mm, width of 175 mm and depth of 60 mm. Link slab specimen had debond zone length (330 mm) equal to roughly 2.5% of both adjacent spans while transition zone length was 150 mm. Three 6 mm bars (reinforcement ratio of 0.01%) were provided as longitudinal reinforcements.

Transverse reinforcements were provided with 6 mm bars at 210 mm c/c. Eight 10 mm shear studs were installed in two rows at each end of the steel I-beam connecting concrete deck. Same EC and SCC mixtures described earlier were used to make link slab specimens. For all link slab specimens, adjacent bridge decks (end parts) were cast with SCC. For SCC link slab specimens (LS-SCC), link slab portion was cast with SCC. For EC link slab specimens (LS-EC), link slab portion was cast with EC (Fig. 6).

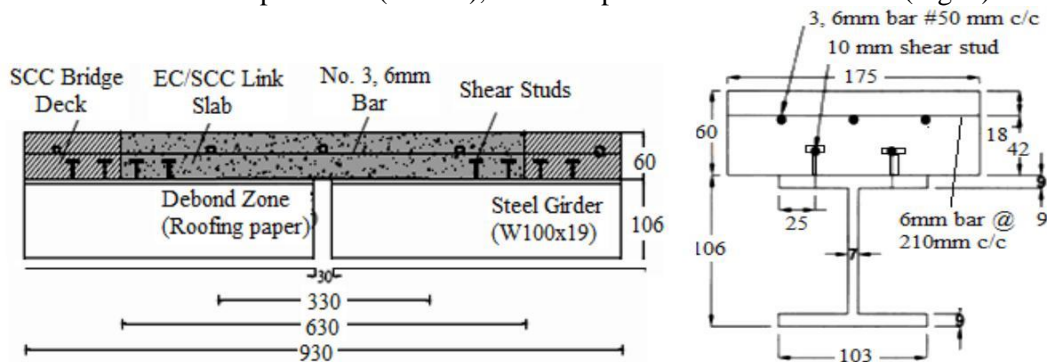


**Figure 6: Geometry and reinforcement details of link slab specimens (Dimensions in mm)**

For all link slabs, the bridge deck part was cast initially and left for setting for 24 hours. After 24 hours, the link slab zone was cast with EC or SCC. Control specimens in the form of cylinders and beams were also cast. Specimens were cured for 28 days at the laboratory conditions while covered with burlap. The relative humidity and the temperature of the laboratory were  $45 \pm 5\%$  and  $24 \pm 2^\circ\text{C}$ , respectively. Fig. 7 shows link slab specimens after casting. The mean compressive strength of EC and SCC were 46 MPa and 48 MPa, respectively while the mean flexural strength were 7.1 MPa and 5.1 MPa.

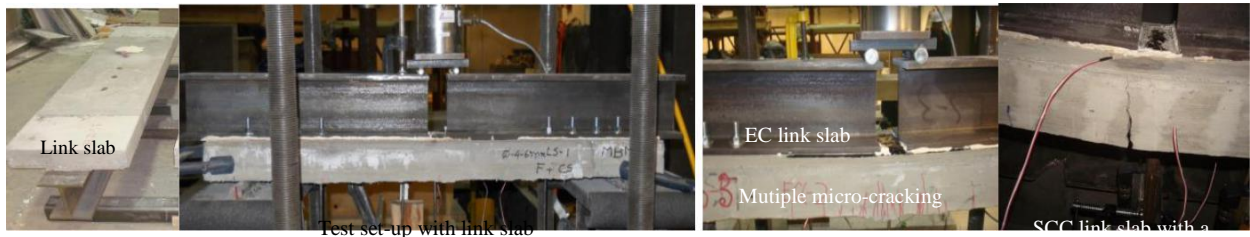


**Figure 7: Link slab, test-setup, and instrumentation and failure modes**

### 2.2.2 Test set-up, instrumentation and testing

Link slab specimens were tested under monotonic loading simulating actual loading and support conditions of the real bridge structure. The test set-up is shown in Fig. 7 where 930 mm long simply supported specimens having effective span of 870 mm were tested, apart. The strain gauges and LVDTs were installed at the centre of the specimen to monitor bar/concrete strain development and displacement. The load was applied through a hydraulic actuator at the centre of the test specimen until failure (Fig. 7). During testing, the load, displacements and strains in concrete and reinforcing steel were monitored along with the observation of crack propagation, failure modes, number of cracks and crack width.

### 2.2.3 Analysis of structural performance of link slabs

SCC link slab (LS- SCC) failed due to the formation of one major crack at the centre of the slab while multiple micro-cracks (crack widths remained below  $50 \mu\text{m}$ ) formed and propagated across the length of the link slab for EC link slab (LS-EC) (Fig. 7). All cracks were observed in the debonding zone only and no crack formed in the deck slab or in the transition zone.

Load-midspan deflection responses of NC and EC link slab specimens showed significant differences (Fig. 8-left). EC link slab clearly showed ductile behaviour with strain hardening as evident from the steady

increase in deformation with the increase in load. SCC link slab failed to show similar strain hardening behaviour. During the loading history, a sudden drop of load was observed at the first peak

followed by the formation of a major crack at the centre in the debonding zone (Fig. 8-left). The load then increased until a second peak was reached with additional deflection. This post-first peak response with large crack width may be associated with the transfer of load to the steel reinforcement (bridging the crack) through steel-NC bond mechanism. The post first peak response in NC link slab associated with single crack formation and large crack width is not acceptable for the link slab application.

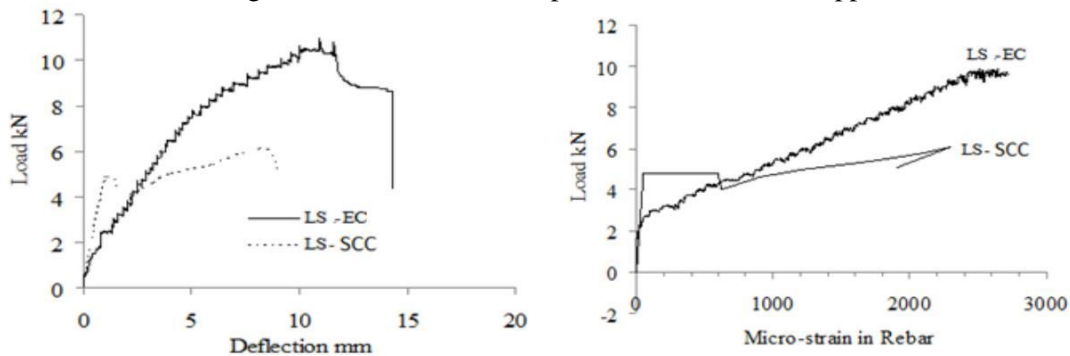


**Figure 8: Comparison of load-deflection and load-rebar strain responses of link slabs**

Load-rebar strain response of the SCC link slab in Fig. 8-right) shows sudden transfer of load to steel reinforcement at the onset of major crack development at the centre (at first peak) and subsequent large strain (stress) development in steel at lower load compared to its EC counterpart. Such stress concentrations in the reinforcement are nonexistent even as the EC link slab was experiencing micro-crack damage. Subsequently, the yielding of rebar occurred at higher load in the EC matrix compared with NC matrix as evident from rebar strain development (Fig. 8-right). The superior strain hardening capacity of EC link slab can be attributed to the absence of shear lag between reinforcing bars and the surrounding VA-EC while the fracture of NC causes unloading of concrete and transfer of load to the reinforcement resulting in high interfacial shear/bond forces causing failure.

The ultimate load of EC link slab (10.7 kN is much higher than that of NC (first peak of 4.8 kN and 2<sup>nd</sup> peak 6.14 kN- Fig 7-left). Based on first peak, the ductility (strain hardening capacity) of the EC links slab is significantly higher as evident from the large deflection of 11.2 mm compared to only 1.9 mm of SCC. The energy absorbing capacity of EC link slab (calculated by the area under the load-deflection curve) was 124 joules compared to 56 joules of its SCC counterpart. While in terms of cracking, EC link slab developed 48 micro-cracks compared to one major crack in SCC link slab.

### 3. Conclusions

The following conclusions are drawn from the study:

EC flexural frames showed better performance compared to their SCC counterparts in terms of ductility (83% higher), ultimate load capacity (30% higher), micro-cracking characteristics with tight crack width less than 100 $\mu$ m and strain-hardening behavior due to fiber bridging.

EC link slabs exhibited superior strain hardening behavior over their SCC counterparts. The inferior strain hardening capacity of SCC link slab can be attributed to the brittle fracture of SCC causing high interfacial shear and subsequent rebar-concrete interfacial bond forces. This resulted in higher rebar strain in SCC link slab (at lower load level). On the other hand, formation of micro-cracks in EC due to fiber bridging action reduces rebar strain leading to stable strain hardening behaviour suitable for link slab applications.

Over all, EC frames and link slabs showed better performance in terms of higher ultimate strength, higher ductility, better energy absorption capacity, large number of micro-crack formation and small crack width development compared with their SCC counterparts.

The study confirmed the viability of constructing link slabs and frames using EC to construct joint-free bridge decks and buildings with enhanced structural performance.

## 4. Acknowledgement

Author acknowledges the financial support of Natural Science and Engineering Research Council (NSERC) Canada.

## 5. References

- Alampalli, S., and Yannotti, A. P. (1998), "In-Service Performance of Integral Bridges and Joint less Decks", *Transportation Research Record* 1624, Paper No. 98-0540, 1-7.
- Caner, A. and Zia, P. (1998), "Behavior and Design of Link Slabs for Joint less Bridge Decks", *PCI Journal*, 43, 68–80.
- Hossain, K.M.A. (2013), "Effect of Air Entrainment and Volcanic Ash on the Properties of Self-consolidating Concrete", *European Journal of Scientific Research*, 95(3) 387-399.
- Hossain, K.M.A., Gahtrehsamani, S. and Anwar, M.S. (2015) "Flexural fatigue performance of ECC link slabs for bridge deck applications", Sustainable Bridge Structure, (Ed. K M Mahmoud), Chapter 22, *CRC Press-Balkema, Taylor & Francis Group*, EH Leiden, The Netherlands, pp. 247-260.
- Hossain, K.M.A. and Anwar, M.S. (2014), "Properties of Green Engineered Cementitious Composites incorporating Volcanic Materials", Proc. Structural Faults & Repair, 8-10 July, Imperial College, London, UK.
- Fischer, G. and Li, V. C. (2003), "Design of Engineered Cementitious Composites (ECC) for processing and workability requirement, Vol. 7, *BMC*, Poland, 29–36.
- Gilani, A. (2001), "Link Slabs for Simply Supported Bridges, incorporating Engineered Cementitious Composites", MDOT SPR-54181. *Structural Research Unit, MDOT, USA*.
- Lepech, M. D. and Li, V. C. (2009), "Application of ECC For Bridge Deck Link Slabs". *RILEM Journal of Materials and Structures*, 42(9)1185-1195.
- Li, V.C. (1993), "From Micromechanics to Structural Engineering –the Design of Cementitious Composites for Civil Engineering Applications", *ASCE Journal of Structural Mechanics and Earthquake Engineering*, 10(2) 37-48.
- Li, V.C. (1998), "Engineered Cementitious Composites - tailored composites through micromechanical modeling", In: Banthia N, Bentur AA, Mufti A, editors. Fiber reinforced concrete: present and the future. Montreal: *Canadian Society for Civil Engineering*, 64-97.
- Li, V. C., Wang, S., Ogawa, A. and Saito, T. (2002), "Interface Tailoring for Strain- Hardening PVA-ECC", *ACI Materials Journal*, 99(5) 463–472.
- Li, V.C. (2003), "Engineered Cementitious Composites (ECC) - A Review of the Material and Its Applications", *Journal of Advanced Concrete Technology*, 1(3) 215–230.
- Li, V.C. and Kanda, T. (1998), "Engineered Cementitious Composites for Structural Applications", *ASCE J. Materials in Civil Engineering*, 10(2), 66-69.
- Ozbay, E.M., Lachemi, M., Karahan, O., Hossain, K.M.A. and Atis, C.D. (2012), "Investigation of the Properties of ECC Incorporating High Volumes of Fly Ash and Metakaolin", *ACI Materials Journal*, 109(5) 565-571.
- Sahmaran, M., Lachemi, M., Hossain, K.M.A., Ranade, R. and Li, V.C. (2010), "Internal Curing of ECCs for Prevention of Early Age Autogenous Shrinkage Cracking", *Cement Concrete Research*, 39(10)893-901.
- Şahmaran, M., Lachemi, M., Hossain, K.M.A. and Li, V.C. (2009), "Influence of Aggregate Type and size on the ductility and mechanical properties of ECC", *ACI Materials Journal*, 106(3)308-316.
- Wang, S. and Li, V.C. (2007), "Engineered Cementitious Composites with high-volume fly ash," *ACI Materials Journal*, 104(3) 233-241.
- Wolde-Tinsae, A. M., and Klinger, J. E. (1987), "Integral Bridge Design and Construction", Report FHWA/MD-87/04, *Maryland Department of Transportation*, USA.
- Zia, P., Caner, A. and El-Safte, A. (1995), "Jointless Bridge Becks Research Project 23241-94-4", *Center for Transportation Engineering Studies, North Carolina State*, pp. 1-117.
- The Ninth International Conference on Construction in the 21<sup>st</sup> Century (CITC-2017)*  
"Revolutionizing the Architecture, Engineering and Construction Industry through Leadership, Collaboration and Technology"